U-Pb geochronology of granitoids in the north-western boundary of the Xolapa Terrane

Victor A. Valencia[1,*], Mihai Ducea[1], Oscar Talavera-Mendoza[2], George Gehrels[1], Joaquin Ruiz[1], and Sarah Shoemaker[1]

[1]*University of Arizona, Department of Geosciences,*
Tucson, Arizona 85721, USA.
[2]*Unidad Académica Ciencias de la Tierra, Universidad Autónoma de Guerrero,*
A.P. 197, 40200 Taxco, Guerrero, Mexico.
**victorv@email.arizona.edu*

ABSTRACT

The Sierra Madre del Sur, a Mesozoic-Cenozoic magmatic arc in southern Mexico, was studied using U-Pb zircon geochronology. Undeformed to slightly deformed plutons from two transects were sampled at the limit between the Guerrero and Xolapa terranes, in order to constrain the magmatic history, nature of the basement and terrane boundaries. Four samples from the Zihuatanejo, Guerrero, transect within the Guerrero terrane, yielded crystallization ages of 41.8 ± 1.4, 43.4 ± 1.6, 40.8 ± 1.4 and, 41.8 ± 4.6 Ma. No inherited zircons were detected in these plutons indicating that pre-existing zircons from continental basement or sediments are not a significant component in these rocks. Five samples from the Atoyac, Guerrero transect within the Xolapa terrane, yielded crystallization ages of 53.5 ± 1.9, 52.7 ± 1.9, 57.3 ± 2.2, 54.4 ± 1.7, and 57.0 ± 2.1 Ma, analogous to the ages reported for the Acapulco intrusive. One sample of this transect yielded an age of 40.2 Ma with an inherited component of 58–64 Ma, similar to the ages determined for the first five samples. Several clusters of Mesozoic inherited zircons with ages of 72–74 Ma, 83–87 Ma, 90–92 Ma, 105–111 Ma and, 143–153 Ma, indicate that the magmatism in the Xolapa terrane was active since the Jurassic, and that multiple episodes of magmatism occurred during the Cretaceous. Inherited zircons also indicate that processes of assimilation and recycling of previous intrusive bodies have played an important role in the evolution of the Xolapa Complex. Older Paleozoic (~320 Ma; ~360 Ma) and Grenvillian (~960–1085 Ma) inherited zircons ages suggest an affinity of the Xolapa Complex with the Acatlán and Oaxaca Complexes, even though the metasedimentary basement of the Xolapa complex (of unknown age) may be the source of these Paleozoic and Grenvillian zircons. The presence of inherited zircons in the Atoyac transect suggests that the limit between the Xolapa and Guerrero terranes is located between these two transects.

Key words: U-Pb, zircon, arc magmatism, Xolapa, Mexico.

RESUMEN

The Sierra Madre del Sur, a Mesozoic-Cenozoic magmatic arc in southern Mexico, was studied using U-Pb zircon geochronology. Undeformed to slightly deformed plutons from two transects were sampled at the limit between the Guerrero and Xolapa terranes, in order to constrain the magmatic history, nature of the basement and terrane boundaries. Four samples from the Zihuatanejo, Guerrero, transect within the Guerrero terrane, yielded crystallization ages of 41.8 ± 1.4, 43.4 ± 1.6, 40.8 ± 1.4 and, 41.8 ± 4.6 Ma. No inherited zircons were detected in these plutons indicating that pre-existing zircons from continental basement or sediments are not a significant component in these rocks. Five samples from the

Atoyac, Guerrero transect within the Xolapa terrane, yielded crystallization ages of 53.5 ± 1.9, 52.7 ± 1.9, 57.3 ± 2.2, 54.4 ± 1.7, and 57.0 ± 2.1 Ma, analogous to the ages reported for the Acapulco intrusive. One sample of this transect yielded an age of 40.2 Ma with an inherited component of 58–64 Ma, similar to the ages determined for the first five samples. Several clusters of Mesozoic inherited zircons with ages of 72–74 Ma, 83–87 Ma, 90–92 Ma, 105–111 Ma and, 143–153 Ma, indicate that the magmatism in the Xolapa terrane was active since the Jurassic, and that multiple episodes of magmatism occurred during the Cretaceous. Inherited zircons also indicate that processes of assimilation and recycling of previous intrusive bodies have played an important role in the evolution of the Xolapa Complex. Older Paleozoic (~320 Ma; ~360 Ma) and Grenvillian (~960–1085 Ma) inherited zircons ages suggest an affinity of the Xolapa Complex with the Acatlán and Oaxaca Complexes, even though the metasedimentary basement of the Xolapa complex (of unknown age) may be the source of these Paleozoic and Grenvillian zircons. The presence of inherited zircons in the Atoyac transect suggests that the limit between the Xolapa and Guerrero terranes is located between these two transects.

Key words: U-Pb, zircon, arc magmatism, Xolapa, Mexico.

INTRODUCTION

The Xolapa Terrane (Campa and Coney, 1983), also known as the Chatino Terrane (Sedlock *et al*., 1993) is a long belt of high grade metamorphic and plutonic rocks of Proterozoic to Cenozoic age facing the Pacific coast in the states of Guerrero and Oaxaca in the Sierra Madre del Sur, Mexico (Figure 1). The origin of this terrane is in debate and has been interpreted as an allochtonous magmatic arc accreted during Late Cretaceous-Early Tertiary time (Campa and Coney, 1983; Coney, 1983), whereas an autochtonous magmatic arc origin has been proposed by others (*i.e*., Ratschbacher *et al*.,1991; Morán Zenteno, 1992; Hermann *et al*. 1994; and Ducea *et al*. 2004).

Due to widespread Cenozoic volcanic cover, intrusive rocks and abundant vegetation, the precise location of the boundary between the Xolapa and the Guerrero terranes is also unclear. Campa and Coney (1983) and Coney and Campa (1987) placed this boundary between Zihuatanejo and Petatlán. Meschede *et al*. (1997) characterized this limit as a normal fault with the hanging wall moving to the northwest as registered by mylonites and ultramylonites. On the other hand, Sedlock *et al*. (1993) placed the boundary between the Guerrero and Xolapa terranes following the trace of the Papalutla fault, which according to these authors is the limit between the Guerrero and Mixteco terranes (Figure 1). They argue that this limit is obscured by Tertiary granites emplaced in the contact between both terranes in the area east of Petatlán (Sedlock *et al*., 1993) or between Petatlán and Atoyac (Tolson *et al*., 1993).

At present, most geochronological data obtained in the Xolapa terrane has been obtained from Rb-Sr and K-Ar mineral data (*e.g.*, Guerrero-García, 1975; Morán-Zenteno, 1992; Schaaf *et al*., 1995) that may not necessarily reflect the crystallization age of plutons but rather their cooling history defined by through their respective closure temperatures. Some valuable U-Pb zircon multifraction data has been obtained in different areas (Robinson *et al*., 1989; Herrmann *et al*., 1994; Schaaf *et al*., 1995). Ducea *et al*. (2004) obtained U-Pb single zircon ages of plutonic and metaplutonic rocks from three transects south of Acapulco using LA-MC-ICPMS. Recently, Solari *et al*. (2007) reported ID-TIMS U-Pb ages of metaplutonic rocks from the Tierra Colorada-Acapulco sector.

The aim of this study is to present new LA-MC-ICPMS U-Pb data for rocks from Atoyac de Álvarez and Zihuatanejo-Altamirano transects in order to document the crystallization ages of plutonic rocks, to constrain the nature of the basement, and to precisely locate the boundary between the Guerrero and Xolapa terranes.

GEOLOGICAL SETTING

The Xolapa Terrane (Campa and Coney, 1983) is a fault-bounded crustal block located in the Pacific margin of southern Mexico (Figure 1). It is bounded by the late Mesozoic Guerrero arc terrane and by the Proterozoic to Mesozoic Mixteco and Oaxaca terranes (Figure 2a). The Xolapa terrane mainly includes orthogneiss, paragneiss and rare marble of Proterozoic to Mesozoic age, which experienced regional deformation, amphibolite facies metamorphism and migmatization, and intrusion by undeformed, mid-Tertiary calc-alkaline granites (De Cserna, 1965; Herrmann *et al*., 1994; Morán-Zenteno *et al*., 1996; Ducea *et al*., 2004; Corona-Chávez *et al*., 2006; Solari *et al*., 2007). The high-grade metamorphism and migmatization is early Tertiary (65–46 Ma; Herrmann *et al*., 1994). Extensional deformation and uplift of southern Mexico occurred during the mid-Tertiary (30–25 Ma; Morán-Zenteno *et al*., 1996; Meschede *et al*., 1997). The northern boundary of the Xolapa terrane was mapped as a belt of mylonites with a normal-fault geometry (Ratschbacher *et al*., 1991; Riller *et al*., 1992, Herrmann, 1994). The other limits are still poorly understood.

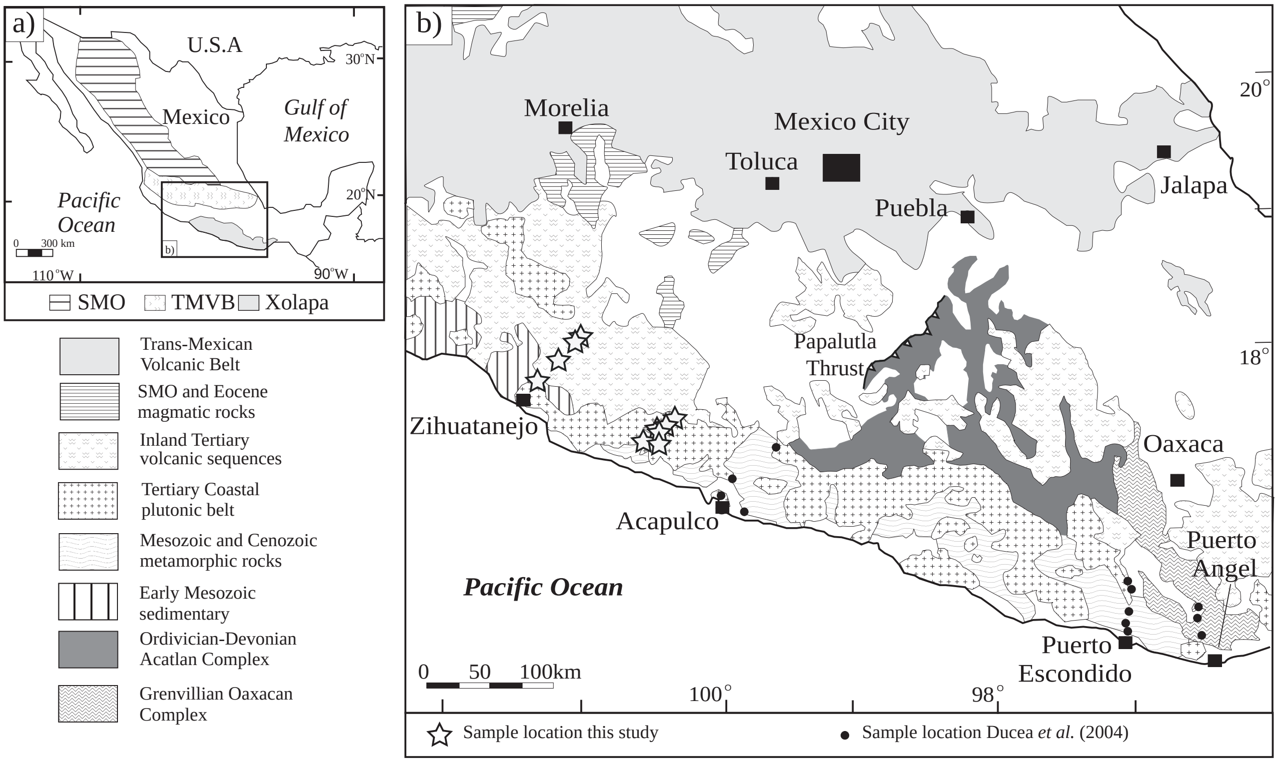

Figure 1. a) Magmatic provinces of Mexico. SMO: Sierra Madre Occidental, TMVB: Trans-Mexican Volcanic Belt. b) Simplified geologic map of southern Mexico (modified after Morán-Zenteno *et al.*, 1996, Morán-Zenteno *et al.*, 1999 and Ortega Gutiérrez *et al.*, 1999). Locations of samples collected for U-Pb geochronology (stars); samples from Ducea et al., 2004 (solid circles) are also shown.

ANALYTICAL METHOD

Around 10 kg sample of igneous rocks were collected at sites shown in Figures 1 and 2, and crushed and milled. Heavy mineral concentrates of the <350 microns fraction were separated magnetically. Inclusion-free zircons from the non-magnetic fraction were then handpicked under a binocular microscope. When possible at least fifty zircons from each sample were mounted in epoxy and polished for laser ablation analyses. Single zircon crystals were analyzed in a VG isoprobe multi-collector ICPMS equipped with nine Faraday collectors, an axial Daly detector, and four ion-counting channels (Gehrels *et al*., 2008). The isoprobe is equipped with an ArF Excimer laser, which has an emission wavelength of 193 nm. The analyses were conducted on 35 or 50 micron spots with an output energy of ~32 mJ and a repetition rate of 8 Hz. Each analysis consisted of one 20-second integration of background on peaks with no laser firing and twenty 1-second integrations on peaks with the laser firing. The depth of each ablation pit was ~15 microns. The collectors were configured to simultaneously measure ^{204}Pb in an ion-counting channel, while ^{206}Pb, ^{207}Pb, ^{208}Pb, ^{232}Th, and ^{238}U are measured with Faraday collectors. All analyses were conducted in static mode. Inter-element fractionation was monitored by analyzing fragments of SL-1, a large concordant zircon crystal from Sri Lanka (SL-1) with a known (ID-TIMS) age of 563.5 ± 3.2 Ma (2σ) (Gehrels *et al*., 2008). The reported ages for zircon grains are based on ^{206}Pb/^{238}U ratios because errors of the ^{207}Pb/^{235}U and ^{206}Pb/^{207}Pb ratios are significantly greater. This is due primarily to the low intensity (commonly <1 mV) of the ^{207}Pb signal from these young, low-U grains. The ^{206}Pb/^{238}U ratios are corrected for common Pb by using the measured ^{206}Pb/^{204}Pb, and the common Pb composition (Stacey and Kramers, 1975) with an uncertainty of 1.0 unit on the assigned common ^{206}Pb/^{204}Pb (Gehrels *et al*., 2008).

Zircons were studied optically under SEM in backscattered electron (BSE) mode and cathodoluminescence (CL) images. Almost all zircons that yielded Cenozoic ages display igneous morphologies (*e.g.*, euhedral crystals). Older zircons are generally smaller, rounded grains with overgrowths, which possibly indicates an inherited origin (Figure 3).

Ages from 5–25 zircon grains were measured from each sample. Results are reported in Table 1 where each line represents a spot analysis. The weighted mean of individual analyses were calculated according to Ludwig (2003). The mean age (Mean) considered only the measurement or random errors (errors in ^{206}Pb/^{238}U and ^{206}Pb/^{204}Pb of each unknown). For these samples the random error are 0.7–1.7 Ma (2σ), and represents ~1–2.9% of the age.

Age of standard, calibration correction from standard, composition of common Pb, decay constant uncertainty are the other sources that contributed to the error in the final

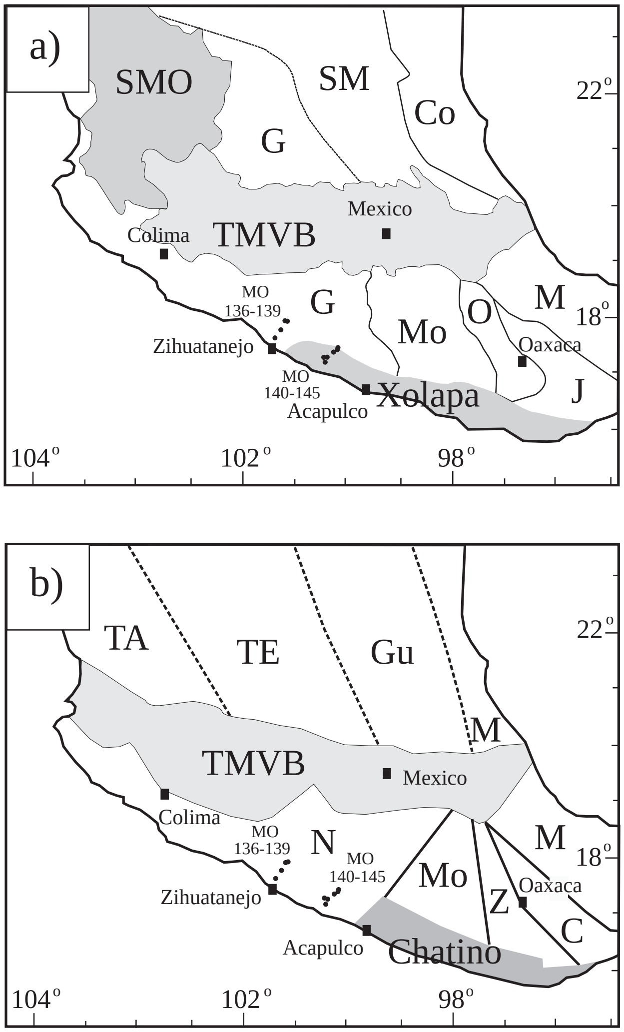

Figure 2. Tectonostratigraphic terranes of central-south of Mexico, samples location from the two transects are shown as solid dots. a) Campa and Coney (1983) configuration. SMO: Sierra Madre Occidental, TMVB: Trans Mexican Volcanic Belt, G: Guerrero Terrane, Mo: Mixteco Terrane, SM: Sierra Madre, O: Oaxaca, J: Juarez., M: Maya, Co: Coahuila. b) Sedlock *et al.* (1993) tectostratigraphic terrane configuration. N: Nahuatl, Mo: Mixteco, Z: Zapoteco, C: Cuitateco, M: Maya, TA: Tahue, TE: Tepehuano, Gu: Guachichil, Chatino=Xolapa.

age determination. These uncertainties are grouped and are known as the systematic error. For these samples the systematic error is ~1.2–2.0%. The error of the age for the sample is calculated adding quadratically the two components (random or measurment error and systematic error). All age uncertainties are reported at the 2-sigma level (2σ).

RESULTS

The plutonic rocks studied here are characterized by medium- to coarse-grained hypidiomorphic granular textures. The samples range in composition from quartz-monzodiorite to granite (Figure.4) and can be divided into two groups which correlate with the two studied transects. Rocks from the Atoyac transect consist exclusively of granites, whereas rocks from the Zihuatanejo transect consist of quartz monzodiorites, granodiorites and granites (Figure.4). Both groups are dominated by quartz, plagioclase, biotite, hornblende and magnetite in different proportions. Biotite is the principal mafic phase in the leucocratic rocks (Atoyac transect), whereas hornblende and biotite are abundant in the less silicic rocks of the Zihuatanejo transect.

Zihuatanejo transect

Four samples were analyzed from the Zihuatanejo transect (Table 2 and Figures 1 and 2). The rocks contain euhedral zircons that have typical igneous morphologies: prominent sharp pyramidal terminations, clear, transparent, and no detectable optical zoning. Their low U/Th ratios (<3) are consistent with a magmatic origin (Rubatto, 2002). The resulting $^{206}Pb/^{238}U$ ages are 41.8 ± 1.4 Ma (n=5, MSWD=1.6) for MO136; 43.4 ± 1.6 Ma (n= 17, MSWD =1.4) for MO137; 40.8 ± 1.4 Ma (n=20, MSWD =1.4) for MO138; and a concordant age of 41.8 ± 4.6 Ma (individual zircons are 39.1 ± 3.8 Ma and 45.1 ± 3.4 Ma) for MO139 (Figure 5). There are no inherited zircons in any of the analyzed samples. Overall, these ages are slightly older than the 37.4 to 40.5 Ma K-Ar ages in biotite-chlorite separates obtained by Stein *et al*. (1994) from similar units.

Atoyac transect

Six samples from the Atoyac transect were analyzed (Figure 1 and Table 2). Sample MO140 yielded a $^{206}Pb/^{238}U$ age of 53.5 ± 1.9 Ma (n=22 zircons, MSWD=2.7) with no inherited grains (Figure 6). Sample MO141 has a $^{206}Pb/^{238}U$ age of 52.7 ± 1.9 Ma (n= 14 zircons, MSWD=4.0). One zircon contains an inherited core of Carboniferous age (326 Ma). Sample MO142 has a $^{206}Pb/^{238}U$ age of 57.3 ± 2.2 Ma (n=13 zircons, MSWD=2.0); inherited cores yielded ages of ~70 Ma, ~90 Ma, 385 Ma and 1085 Ma. Sample MO143 has a $^{206}Pb/^{238}U$ age of 54.4 ± 1.7 Ma (n=17 zircons, MSWD=1.2), with inherited cores of ~100 Ma, (n=3), ~150 Ma, (n=3), 960 Ma and 1848 Ma. Sample MO144 has a $^{206}Pb/^{238}U$ age of 57.0 ± 2.1 Ma (n=13 zircons, MSWD=2.4) with a Late Cretaceous (~85 Ma, n=4) inherited component. Sample MO145 has a $^{206}Pb/^{238}U$ age of 40.2 ± 2.1 Ma (n = 14 zircons, MSWD=2.4); inherited components in this sample are ~60 (n=6), ~110 Ma (n=2) and 1024 Ma (n=1).

DISCUSSION

Granitic rocks from Zihuatanejo have mid-Tertiary (43–40 Ma) crystallization ages with no inherited components. Although it is well known that the region is under-

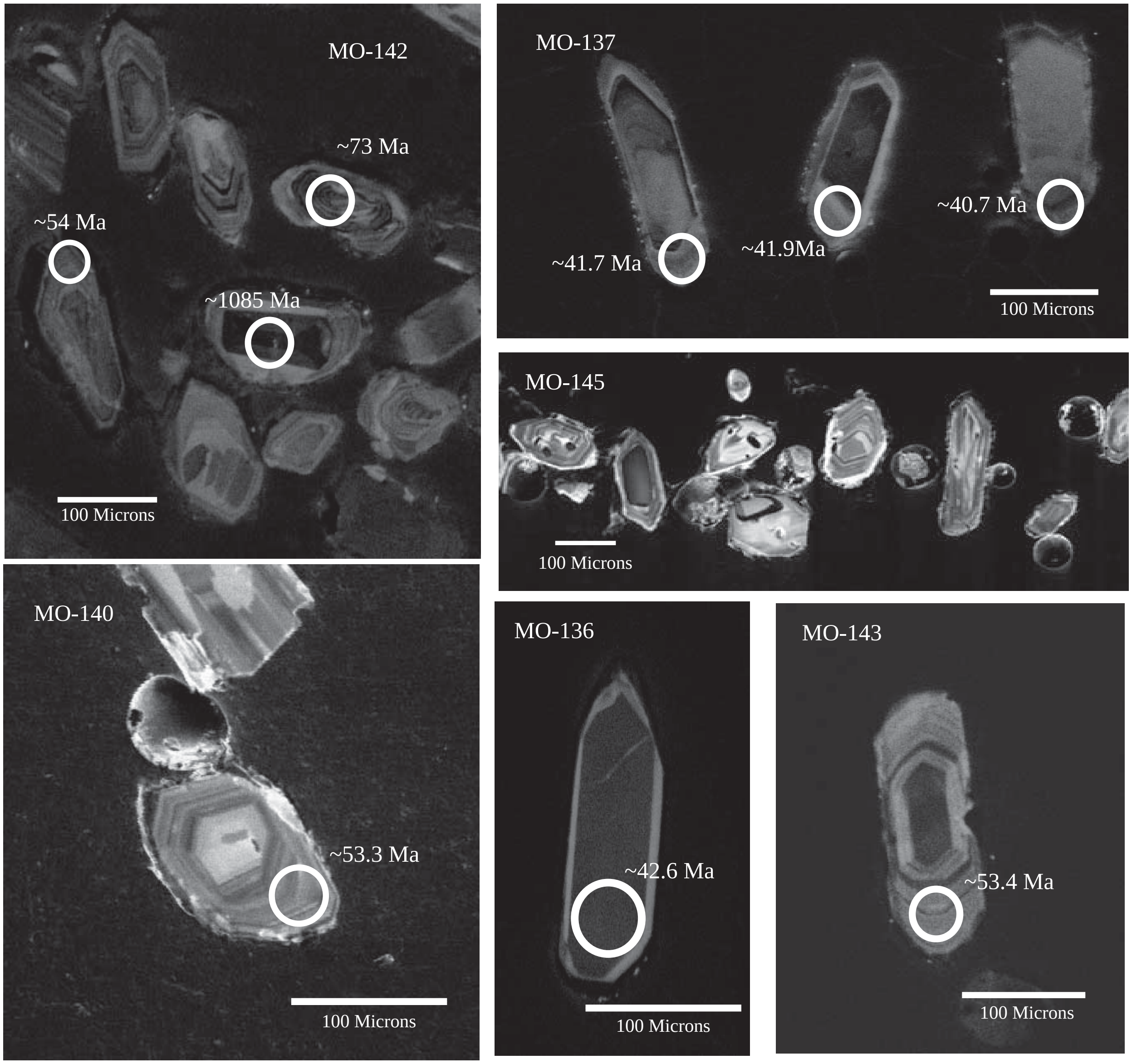

Figure 3. Zircon cathodoluminisence microphotographs. Variation in growth zoning from broad to narrow in magmatic zircons (MO136, MO137, MO140, MO143). Zircons with xenocrystic cores (MO142 y MO145).

lain by modified oceanic crust containing old (Archean to Paleozoic) zircons of the Arteaga Complex (Centeno-Garcia *et al*., 1993; Talavera *et al*., 2007), the absence of inherited old grains indicates that crustal contamination was not a significant process in the genesis of mid-Tertiary granitic magmas near Zihuatanejo.

On the other hand, most granitic plutons at Atoyac, Guerrero yielded 52.7–58.1 Ma crystallization ages. Only one granitic pluton in this transect has a younger, 40 Ma age. Younger Rb-Sr biotite-whole rocks ages have been obtained from the Atoyac transect (*e.g.*, 28.3 ± 0.6 Ma, Schaaf *et al*., 1995, but there are also comparable K-Ar ages from the Instituto Mexicano del Petróleo, IMP), indicative for a prolonged thermal event in that area (Schaaf, written communication).

The former are identical in age to the Acapulco granite dated at 55 Ma (Ducea *et al*., 2004) whereas the later is within the range recorded in plutons at Zihuatanejo. Regardles of their age, granitic plutons at Atoyac also contain abundant inherited zircon grains with ages ranging from 58 to 1085 Ma. Major clusters of inherited zircon are early Tertiary (58–64 Ma), mid- to Late Cretaceous (72–111 Ma), Jurassic (143–153 Ma), mid-Paleozoic (320–360 Ma) and Mesoproterozoic (960–1085 Ma). Rocks with zircons of such age are widespread in the Acatlán and Xolapa complexes (Keppie *et al*., 2004; Talavera *et al*., 2005), but they are not found in the Guerrero Terrane (Talavera *et al*., 2007). It is not possible to discern which of these two complexes is the source of inherited zircons recorded in granitic plutons at Atoyac given the limited available data.

Table 1. LA-MC-ICPMS U-Pb zircon data of samples from the Atoyac and Zihuatanejo transects.

	Concentration				Isotopic Ratio							Apparent ages					
Sample	U (ppm)	Th (ppm)	U/Th	$U^{206}Pb_m/^{204}Pb_c$	$^{207}Pb/^{235}U$	±%	$^{206}Pb/^{238}U$	±%	Error corr	$^{206}Pb/^{207}U$	±%	$^{206}Pb/^{238}U$	±Ma	$^{207}Pb/^{235}U$	±Ma	$^{207}Pb/^{206}Pb$	±Ma
MO136																	
MO136-1	607.4	849.6	0.7	404	0.0429	41.69	0.0066	4.11	0.10	21.15	41.48	42.31	1.74	42.69	18.01	63.86	493.97
MO136-2	933.7	1231.6	0.8	931	0.0383	27.67	0.0064	2.52	0.09	23.19	27.55	41.43	1.05	38.20	10.72	NA	NA
MO136-5	1112.3	1373.6	0.8	984	0.0418	25.81	0.0066	2.22	0.09	21.68	25.72	42.24	0.94	41.59	10.90	4.12	309.73
MO136-6	649.8	436.8	1.5	418	0.0512	42.10	0.0066	7.41	0.18	17.83	41.44	42.57	3.16	50.73	21.67	455.50	459.79
MO136-7	616.5	596.5	1.0	129	0.0440	69.79	0.0060	7.98	0.11	18.83	69.33	38.59	3.09	43.69	30.69	333.64	785.89
MO137																	
MO137-1	75.3	48.6	1.5	61	0.0880	55.29	0.0071	7.98	0.14	11.12	54.71	45.61	3.65	85.68	48.26	1424.17	522.49
MO137-2	143.1	105.6	1.4	165	0.0379	76.63	0.0066	7.03	0.09	23.89	76.31	42.17	2.97	37.75	29.05	NA	NA
MO137-4	200.6	100.6	2.0	196	0.0409	68.91	0.0072	4.12	0.06	24.11	68.79	45.97	1.90	40.73	28.24	NA	NA
MO137-5	221.0	136.2	1.6	183	0.0934	41.49	0.0070	6.52	0.16	10.32	40.98	44.93	2.94	90.66	38.60	1564.44	384.07
MO137-6	259.8	157.5	1.6	202	0.0393	63.35	0.0070	5.55	0.09	24.68	63.11	45.15	2.52	39.10	24.95	NA	NA
MO137-7	396.3	301.8	1.3	199	0.0769	45.16	0.0065	9.27	0.21	11.60	44.20	41.55	3.86	75.19	34.65	1343.16	426.88
MO137-8	242.6	171.6	1.4	257	0.0634	49.01	0.0068	8.38	0.17	14.87	48.29	43.89	3.69	62.38	31.05	845.98	502.23
MO137-9	369.2	325.2	1.1	412	0.0532	39.52	0.0069	7.10	0.18	17.82	38.88	44.17	3.15	52.63	21.13	456.97	431.27
MO137-10	395.7	297.4	1.3	37	0.1768	43.78	0.0068	8.58	0.20	5.33	42.93	43.93	3.78	165.33	75.71	2720.70	353.75
MO137-13	609.8	620.6	1.0	234	0.0719	44.12	0.0064	10.58	0.24	12.29	42.83	41.17	4.37	70.46	31.69	1229.74	420.36
MO137-14	292.3	270.8	1.1	58	0.1116	47.13	0.0064	9.32	0.20	7.91	46.19	41.16	3.85	107.42	52.04	2048.03	408.03
MO137-15	306.9	229.6	1.3	128	0.0373	65.34	0.0063	8.54	0.13	23.29	64.78	40.48	3.47	37.18	24.45	NA	NA
MO137-16	223.6	140.0	1.6	200	0.0854	43.71	0.0067	8.48	0.19	10.78	42.88	42.90	3.65	83.22	37.22	1483.55	406.25
MO137-18	116.9	88.5	1.3	49	0.1107	55.69	0.0064	12.17	0.22	8.00	54.34	41.28	5.04	106.59	60.73	2027.98	481.13
MO137-20	259.6	144.7	1.8	106	0.0593	57.93	0.0066	9.95	0.17	15.44	57.07	42.65	4.25	58.46	34.27	766.11	601.14
MO137-22	179.5	128.7	1.4	180	0.0512	65.65	0.0065	7.58	0.12	17.62	65.21	42.08	3.20	50.73	33.59	481.50	720.24
MO137-23	321.6	185.5	1.7	225	0.0560	48.56	0.0066	3.72	0.08	16.29	48.42	42.55	1.59	55.37	27.26	652.46	519.60
MO138																	
MO138-2	529.2	559.1	0.9	557	0.0503	44.98	0.0067	5.84	0.13	18.24	44.60	42.78	2.50	49.87	22.73	405.12	499.17
MO138-3	350.2	407.4	0.9	322	0.0209	61.77	0.0062	3.46	0.06	41.23	61.67	40.13	1.39	20.99	13.01	NA	NA
MO138-4	385.8	394.1	1.0	380	0.0373	46.97	0.0061	3.59	0.08	22.73	46.83	39.50	1.42	37.16	17.62	NA	NA
MO138-5	412.1	235.9	1.7	313	0.0454	46.95	0.0063	2.71	0.06	19.12	46.87	40.45	1.10	45.07	21.41	298.57	534.65
MO138-6	445.3	568.1	0.8	479	0.0438	37.05	0.0065	3.19	0.09	20.42	36.91	41.72	1.34	43.57	16.36	146.33	432.87
MO138-7	382.2	332.3	1.2	333	0.0201	64.41	0.0065	4.06	0.06	44.73	64.28	41.93	1.71	20.22	13.07	NA	NA
MO138-8	208.6	211.9	1.0	206	0.0536	53.46	0.0063	4.99	0.09	16.28	53.23	40.69	2.04	53.04	28.70	654.28	571.01
MO138-10	337.6	329.6	1.0	210	0.0398	66.20	0.0068	6.97	0.11	23.47	65.83	43.49	3.04	39.59	26.38	NA	NA
MO138-11	345.2	199.7	1.7	206	0.0530	47.20	0.0060	5.33	0.11	15.47	46.90	38.24	2.04	52.48	25.11	763.04	494.29
MO138-12	305.7	336.7	0.9	257	0.0492	46.04	0.0059	5.78	0.13	16.60	45.68	38.06	2.20	48.76	22.74	612.39	493.45
MO138-13	528.8	501.7	1.1	590	0.0403	37.91	0.0062	3.96	0.10	21.14	37.70	39.67	1.58	40.08	15.38	65.13	448.85
MO138-14	374.8	257.5	1.5	389	0.0329	53.07	0.0064	3.52	0.07	26.71	52.95	40.98	1.45	32.89	17.59	NA	NA
MO138-15	342.3	317.7	1.1	211	0.0294	66.07	0.0062	3.51	0.05	29.08	65.98	39.78	1.40	29.38	19.51	NA	NA
MO138-16	581.5	547.8	1.1	343	0.0626	36.41	0.0068	5.72	0.16	14.97	35.96	43.65	2.50	61.61	22.87	830.93	374.87
MO138-18	1023.0	639.0	1.6	878	0.0378	32.94	0.0067	3.19	0.10	24.47	32.78	43.12	1.38	37.70	12.57	-295.63	418.60
MO138-19	288.1	348.9	0.8	452	0.0703	40.87	0.0064	4.32	0.11	12.64	40.65	41.38	1.79	68.95	28.75	1175.43	402.06
MO138-22	663.2	945.9	0.7	740	0.0380	34.52	0.0062	6.23	0.18	22.49	33.95	39.85	2.49	37.88	13.24	NA	NA
MO138-23	1598.2	718.5	2.2	576	0.0597	54.62	0.0064	7.25	0.13	14.79	54.14	41.14	2.99	58.86	32.57	856.68	562.10
MO138-24	267.8	354.2	0.8	330	0.0304	59.29	0.0064	9.70	0.16	29.00	58.49	41.13	4.00	30.44	18.16	NA	NA
MO138-25	571.7	587.5	1.0	608	0.0437	33.50	0.0060	5.85	0.17	19.06	32.98	38.78	2.28	43.38	14.74	306.07	375.70
MO139																	
MO139-1	356.8	126.3	2.8	276	0.0546	45.93	0.0070	7.63	0.17	17.72	45.29	45.08	3.45	53.99	25.15	469.64	501.24
MO139-2	433.7	444.9	1.0	280	0.0497	49.02	0.0061	8.11	0.17	16.86	48.35	39.08	3.18	49.29	24.46	579.16	525.21
MO140																	
MO140-1	386.0	337.1	1.1	262	0.0625	49.46	0.0081	2.47	0.05	17.75	49.40	51.69	1.28	61.58	30.93	465.50	547.15
MO140-3	463.9	319.9	1.5	662	0.0465	44.94	0.0081	4.21	0.09	23.87	44.74	51.73	2.19	46.19	21.02	NA	NA
MO140-4	403.3	97.3	4.1	300	0.0463	51.73	0.0085	4.86	0.09	25.26	51.50	54.45	2.66	45.96	24.03	NA	NA
MO140-5	488.9	190.0	2.6	628	0.0507	35.00	0.0083	4.47	0.13	22.59	34.72	53.29	2.39	50.18	17.85	NA	NA
MO140-6	255.8	89.1	2.9	189	0.0481	61.78	0.0079	6.70	0.11	22.52	61.41	50.48	3.39	47.74	29.76	NA	NA

Table 1 (Continued). LA-MC-ICPMS U-Pb zircon data of samples from the Atoyac and Zihuatanejo transects.

Sample	Concentration				Isotopic Ratio							Apparent ages					
	U (ppm)	Th (ppm)	U/Th	$U^{206}Pb_m/^{204}Pb_c$	$^{207}Pb/^{235}U$	±%	$^{206}Pb/^{238}U$	±%	Error corr	$^{206}Pb/^{207}U$	±%	$^{206}Pb/^{238}U$	±Ma	$^{207}Pb/^{235}U$	±Ma	$^{207}Pb/^{206}Pb$	±Ma
MO140-7	185.7	76.6	2.4	184	0.0535	62.31	0.0077	6.83	0.11	19.81	61.94	49.34	3.38	52.89	33.28	216.78	716.95
MO140-8	166.9	81.5	2.0	184	0.1155	44.36	0.0080	18.83	0.42	9.60	40.17	51.67	9.76	111.01	50.75	1698.95	370.04
MO140-9	156.9	70.3	2.2	204	0.0900	46.14	0.0088	8.90	0.19	13.41	45.28	56.22	5.02	87.52	41.32	1056.26	455.84
MO140-10	175.3	90.5	1.9	204	0.0376	68.45	0.0078	14.62	0.21	28.61	66.87	50.15	7.36	37.52	25.83	NA	NA
MO140-11	180.5	104.6	1.7	176	0.0527	65.42	0.0088	4.76	0.07	22.90	65.25	56.24	2.69	52.20	34.45	NA	NA
MO140-13	128.7	56.2	2.3	164	0.0383	82.81	0.0080	8.94	0.11	28.66	82.33	51.18	4.59	38.20	31.74	NA	NA
MO140-14	155.4	85.9	1.8	113	0.0340	74.88	0.0078	5.34	0.07	31.64	74.69	50.07	2.68	33.93	25.51	NA	NA
MO140-15	143.4	102.5	1.4	190	0.0617	91.71	0.0087	6.09	0.07	19.35	91.51	55.59	3.40	60.80	55.90	271.19	1048.92
MO140-16	140.9	79.3	1.8	223	0.1164	38.04	0.0085	6.11	0.16	10.11	37.54	54.79	3.36	111.84	44.00	1604.26	350.08
MO140-17	178.6	88.7	2.0	122	0.0228	83.89	0.0085	5.86	0.07	51.12	83.69	54.34	3.20	22.92	19.26	NA	NA
MO140-18	643.9	241.3	2.7	515	0.0549	37.57	0.0089	3.08	0.08	22.22	37.45	56.84	1.76	54.32	20.75	NA	NA
MO140-19	205.1	116.7	1.8	260	0.0984	43.63	0.0088	6.44	0.15	12.35	43.15	56.58	3.66	95.34	42.70	1221.37	423.98
MO140-20	210.1	130.5	1.6	277	0.1300	26.67	0.0083	9.75	0.37	8.83	24.82	53.44	5.23	124.11	34.61	1852.74	224.34
MO140-21	148.0	57.6	2.6	242	0.0344	72.58	0.0084	6.75	0.09	33.68	72.27	53.93	3.65	34.34	25.04	NA	NA
MO140-22	161.6	73.3	2.2	256	0.0432	62.35	0.0085	11.52	0.18	27.19	61.28	54.70	6.33	42.96	27.00	NA	NA
MO140-24	473.1	180.3	2.6	665	0.0508	32.83	0.0086	4.00	0.12	23.29	32.59	55.05	2.21	50.29	16.79	NA	NA
MO140-25	194.1	129.4	1.5	238	0.0654	58.22	0.0086	11.25	0.19	18.09	57.12	55.05	6.22	64.28	37.92	423.03	637.40
MO141																	
MO141-2	1270.3	381.0	3.3	1723	0.0549	18.02	0.0083	3.20	0.18	20.80	17.73	53.21	1.71	54.30	10.00	102.58	209.65
MO141-3	431.6	241.6	1.8	579	0.0813	37.04	0.0079	6.23	0.17	13.44	36.52	50.89	3.18	79.35	30.12	1052.01	367.88
MO141-4	675.9	567.1	1.2	653	0.0654	30.15	0.0085	5.07	0.17	17.88	29.72	54.47	2.78	64.37	19.84	449.71	330.10
MO141-5	179.6	23.5	7.6	448	0.0538	60.12	0.0078	20.70	0.34	19.90	56.44	49.89	10.36	53.23	32.33	206.31	654.63
MO141-6	524.0	253.0	2.1	830	0.0597	28.57	0.0082	4.29	0.15	18.96	28.24	52.69	2.27	58.87	17.17	318.15	321.03
MO141-7	919.5	299.5	3.1	932	0.0663	24.77	0.0080	2.78	0.11	16.65	24.62	51.41	1.43	65.18	16.54	605.46	266.25
MO141-8	973.6	422.8	2.3	1167	0.0634	22.04	0.0088	3.26	0.15	19.07	21.80	56.28	1.84	62.41	14.09	304.37	248.40
MO141-9	303.0	89.9	3.4	349	0.0447	52.19	0.0081	3.34	0.06	24.84	52.08	51.75	1.74	44.45	23.44	NA	NA
MO141-10	326.0	36.3	9.0	421	0.0923	43.99	0.0095	20.48	0.47	14.24	38.93	61.14	12.57	89.62	40.40	935.00	399.26
MO141-11	1700.0	1694.5	1.0	980	0.0546	23.26	0.0080	2.78	0.12	20.10	23.09	51.12	1.43	54.00	12.82	183.49	268.90
MO141-12	451.2	238.9	1.9	407	0.0462	52.77	0.0078	3.59	0.07	23.13	52.65	49.81	1.80	45.89	24.48	NA	NA
MO141-13	304.4	155.5	2.0	321	0.0371	57.85	0.0083	8.56	0.15	30.87	57.21	53.29	4.58	36.96	21.55	NA	NA
MO141-15	161.4	40.1	4.0	953	0.3779	23.89	0.0519	6.85	0.29	18.92	22.89	325.87	22.85	325.46	87.75	322.47	259.94
MO141-17	164.4	91.6	1.8	246	0.0875	50.94	0.0084	5.78	0.11	13.23	50.61	53.87	3.13	85.15	44.27	1084.54	507.43
MO141-18	304.1	190.5	1.6	408	0.0407	65.64	0.0091	5.48	0.08	30.92	65.41	58.57	3.23	40.50	26.77	NA	NA
MO141-19	521.9	202.8	2.6	466	0.0667	44.61	0.0085	6.92	0.16	17.47	44.07	54.28	3.77	65.60	29.79	500.89	485.16
MO141-20	204.5	81.1	2.5	225	0.0728	48.49	0.0088	10.24	0.21	16.65	47.39	56.42	5.80	71.36	35.23	606.17	512.51
MO141-21	325.2	166.0	2.0	353	0.0469	56.77	0.0089	5.17	0.09	26.21	56.53	57.22	2.97	46.54	26.68	NA	NA
MO141-23	792.1	486.9	1.6	206	0.0699	44.44	0.0082	2.95	0.07	16.09	44.34	52.37	1.55	68.61	31.07	679.58	473.73
MO141-24	318.0	166.7	1.9	274	0.0809	42.32	0.0090	7.31	0.17	15.42	41.69	58.05	4.26	78.99	34.18	770.12	438.83
MO141-25	175.8	78.9	2.2	123	0.0794	48.84	0.0076	8.08	0.17	13.16	48.17	48.70	3.95	77.61	38.65	1094.45	482.20
MO142																	
MO142-1	218.9	50.7	4.3	269	0.0836	46.37	0.0090	7.78	0.17	14.85	45.72	57.82	4.51	81.56	38.64	848.02	475.29
MO142-2	161.2	28.7	5.6	262	0.0862	50.73	0.0084	6.00	0.12	13.42	50.38	53.89	3.24	83.97	43.47	1054.78	507.30
MO142-3	254.7	17.2	14.8	358	0.0919	34.24	0.0088	6.46	0.19	13.20	33.62	56.49	3.67	89.31	31.47	1088.82	336.84
MO142-4	70.4	22.6	3.1	133	0.1383	67.22	0.0113	5.54	0.08	11.25	66.99	72.31	4.03	131.50	90.24	1402.05	641.77
MO142-5	571.8	45.0	12.7	604	0.0692	42.19	0.0091	7.50	0.18	18.07	41.52	58.20	4.38	67.93	29.22	425.75	463.03
MO142-6	538.0	39.3	13.7	774	0.0602	31.38	0.0095	4.32	0.14	21.79	31.09	61.07	2.65	59.38	19.01	NA	NA
MO142-8	500.7	193.9	2.6	13007	1.7725	5.08	0.1700	4.66	0.92	13.22	2.03		50.85	1035.4	87.57	1085.63	20.31
MO142-9	88.6	51.7	1.7	1005	0.4723	21.30	0.0616	4.36	0.20	17.99	20.85	385.59	17.30	392.79	97.32	435.44	232.10
MO142-10	206.8	73.8	2.8	390	0.0796	43.50	0.0097	7.06	0.16	16.83	42.92	62.29	4.42	77.73	34.55	582.71	466.03
MO142-11	267.7	79.7	3.4	340	0.0746	42.00	0.0099	5.18	0.12	18.21	41.68	63.24	3.29	73.10	31.35	408.80	466.23
MO142-12	611.2	52.0	11.8	353	0.0808	38.37	0.0090	5.73	0.15	15.29	37.94	57.50	3.31	78.91	31.01	787.72	398.24
MO142-13	246.2	55.5	4.4	834	0.1228	28.24	0.0141	7.87	0.28	15.81	27.12	90.12	7.14	117.57	34.60	716.38	287.98
MO142-14	5568.0	117.8	47.3	1265	0.0727	18.52	0.0101	1.71	0.09	19.24	18.45	65.07	1.12	71.24	13.58	283.82	210.96
MO142-15	782.7	100.5	7.8	1826	0.0736	21.39	0.0100	4.73	0.22	18.79	20.86	64.29	3.05	72.07	15.85	338.72	236.20

Table 1 (Continued). LA-MC-ICPMS U-Pb zircon data of samples from the Atoyac and Zihuatanejo transects.

	Concentration				Isotopic Ratio							Apparent ages					
Sample	U (ppm)	Th (ppm)	U/Th	$U^{206}Pb_m/^{204}Pb_c$	$^{207}Pb/^{235}U$	±%	$^{206}Pb/^{238}U$	±%	Error corr	$^{206}Pb/^{207}U$	±%	$^{206}Pb/^{238}U$	±Ma	$^{207}Pb/^{235}U$	±Ma	$^{207}Pb/^{206}Pb$	±Ma
MO142-16	252.0	52.0	4.8	256	0.1375	46.04	0.0111	10.83	0.24	11.13	44.75	71.17	7.75	130.83	62.33	1422.01	427.51
MO142-17	280.3	84.2	3.3	461	0.0829	42.35	0.0103	11.21	0.26	17.09	40.84	65.88	7.42	80.82	35.02	548.54	445.95
MO142-18	234.7	19.8	11.9	450	0.0887	44.70	0.0107	10.65	0.24	16.63	43.41	68.60	7.34	86.27	39.47	607.76	469.33
MO142-19	1912.7	153.1	12.5	3553	0.0579	8.83	0.0090	1.88	0.21	21.44	8.63	57.82	1.09	57.19	5.18	30.66	103.41
MO142-20	515.5	33.0	15.6	541	0.0622	38.21	0.0088	6.92	0.18	19.56	37.58	56.66	3.94	61.29	23.86	246.15	432.69
MO142-21	174.7	53.5	3.3	311	0.0709	77.48	0.0085	8.62	0.11	16.45	77.00	54.29	4.70	69.54	54.29	632.05	829.06
MO142-22	372.5	29.2	12.7	859	0.1006	30.19	0.0144	11.28	0.37	19.72	28.01	92.10	10.46	97.36	30.39	228.15	323.52
MO142-23	208.3	86.9	2.4	321	0.1062	46.49	0.0099	8.83	0.19	12.83	45.65	63.39	5.62	102.48	48.93	1145.15	453.54
MO142-24	333.6	75.6	4.4	640	0.0871	38.26	0.0115	3.61	0.09	18.21	38.09	73.77	2.68	84.84	33.30	408.77	426.06
MO142-25	700.1	124.6	5.6	7354	0.3936	6.14	0.0519	4.24	0.69	18.18	4.45	326.16	14.17	336.96	24.26	412.18	49.69
MO143																	
MO143-1	411.6	377.8	1.1	1025	0.0588	27.45	0.0086	2.76	0.10	20.14	27.31	55.15	1.53	58.04	16.27	179.12	318.37
MO143-2	186.8	90.8	2.1	521	0.0830	81.20	0.0086	6.72	0.08	14.27	80.92	55.13	3.72	80.96	66.22	930.68	830.51
MO143-3	510.2	181.5	2.8	937	0.0673	19.43	0.0084	4.12	0.21	17.25	18.99	54.10	2.24	66.17	13.20	528.10	208.11
MO143-4	860.7	325.3	2.6	2145	0.0611	17.89	0.0086	4.87	0.27	19.36	17.22	55.04	2.69	60.17	11.03	269.69	197.39
MO143-5	125.5	81.4	1.5	614	0.1250	50.04	0.0082	10.96	0.22	9.03	48.82	52.56	5.78	119.64	61.63	1812.39	443.45
MO143-6	854.5	778.7	1.1	2020	0.0596	16.86	0.0083	2.66	0.16	19.13	16.65	53.11	1.42	58.81	10.16	297.59	189.93
MO143-8	224.2	95.3	2.4	961	0.0905	50.52	0.0083	10.56	0.21	12.66	49.41	53.36	5.66	87.99	45.41	1171.57	489.02
MO143-9	302.6	100.2	3.0	1137	0.0813	28.43	0.0083	6.71	0.24	14.10	27.63	53.33	3.59	79.33	23.19	955.85	282.46
MO143-10	51.0	27.5	1.9	476	0.2107	29.58	0.0231	9.07	0.31	15.09	28.15	146.99	13.47	194.18	61.40	814.95	294.26
MO143-11	1091.4	388.6	2.8	3913	0.0581	9.00	0.0084	1.94	0.22	20.00	8.79	54.14	1.06	57.37	5.30	194.63	102.20
MO143-12	387.2	169.3	2.3	2012	0.0369	34.90	0.0083	3.85	0.11	31.08	34.68	53.44	2.07	36.83	13.00	NA	NA
MO143-13	467.5	127.4	3.7	3305	0.0627	23.25	0.0083	3.09	0.13	18.34	23.05	53.58	1.66	61.79	14.71	392.70	258.54
MO143-15	242.9	64.0	3.8	1073	0.1179	36.55	0.0160	6.42	0.18	18.72	35.98	102.39	6.62	113.17	42.84	346.39	406.90
MO143-16	115.1	51.2	2.2	925	0.1967	24.40	0.0224	5.44	0.22	15.72	23.78	142.90	7.85	182.29	47.59	729.34	252.03
MO143-17	201.7	51.6	3.9	2270	0.1214	36.83	0.0166	5.98	0.16	18.85	36.34	106.16	6.39	116.37	44.42	330.42	412.11
MO143-18	750.1	1102.9	0.7	2078	0.0649	13.03	0.0088	3.94	0.30	18.65	12.42	56.31	2.23	63.80	8.54	354.65	140.22
MO143-19	135.1	183.9	0.7	936	0.2110	19.68	0.0245	7.69	0.39	15.98	18.11	155.73	12.11	194.40	41.31	694.37	193.01
MO143-21	356.0	191.6	1.9	1066	0.0774	26.13	0.0088	2.96	0.11	15.72	25.96	56.68	1.68	75.74	20.34	728.38	275.16
MO143-22	481.6	167.4	2.9	2379	0.0564	25.76	0.0083	4.47	0.17	20.33	25.37	53.38	2.39	55.70	14.64	156.96	296.88
MO143-23	234.1	71.4	3.3	557	0.0994	35.19	0.0087	8.64	0.25	12.13	34.12	56.15	4.87	96.25	34.92	1255.97	333.59
MO143-24	26.3	25.6	1.0	2860	2.6862	8.41	0.1747	5.72	0.68	8.97	6.16		64.12	1324.6	206.82	1824.16	55.91
MO143-25	294.2	52.3	5.6	2041	0.0947	27.67	0.0163	3.41	0.12	23.76	27.45	104.33	3.58	91.85	26.25	NA	NA
MO143-25	280.2	136.0	2.1	1260	1.6067	15.27	0.1607	4.66	0.30	13.79	14.54	960.40	48.04	972.83	222.79	1001.02	147.65
MO143-27	295.2	107.7	2.7	1383	0.0869	31.90	0.0084	5.66	0.18	13.28	31.39	53.72	3.05	84.59	27.75	1076.50	315.06
MO143-28	191.9	82.6	2.3	425	0.1279	23.09	0.0085	5.19	0.22	9.21	22.49	54.81	2.86	122.18	29.54	1776.06	205.22
MO144																	
MO144-1	870.7	62.2	14.0	1294	0.0818	22.48	0.0137	3.81	0.17	23.07	22.15	87.64	3.36	79.83	18.50	NA	NA
MO144-3	614.5	38.3	16.1	2961	0.0631	21.95	0.0095	4.05	0.18	20.82	21.57	61.11	2.49	62.11	13.96	100.74	255.06
MO144-4	1058.1	124.0	8.5	1817	0.0584	18.17	0.0087	3.28	0.18	20.48	17.87	55.70	1.84	57.66	10.72	140.11	209.80
MO144-5	458.5	11.7	39.2	2096	0.0741	19.95	0.0096	2.92	0.15	17.89	19.73	61.65	1.81	72.55	14.89	448.72	219.21
MO144-6	952.2	102.2	9.3	1740	0.0523	20.12	0.0089	1.96	0.10	23.46	20.02	57.14	1.12	51.79	10.64	NA	NA
MO144-7	446.0	101.5	4.4	3181	0.0772	28.48	0.0102	14.01	0.49	18.28	24.80	65.62	9.23	75.49	22.08	400.48	277.79
MO144-9	115.5	28.4	4.1	829	0.0795	23.85	0.0095	5.57	0.23	16.42	23.19	60.79	3.40	77.72	19.08	635.44	249.53
MO144-10	129.7	25.5	5.1	1011	0.0701	20.34	0.0094	5.41	0.27	18.47	19.61	60.26	3.27	68.80	14.38	377.10	220.53
MO144-11	2228.5	3043.0	0.7	365	0.0662	47.60	0.0137	4.25	0.09	28.56	47.41	87.88	3.76	65.13	31.53	NA	NA
MO144-12	286.5	67.1	4.3	1277	0.0712	17.78	0.0088	6.86	0.39	17.09	16.40	56.62	3.90	69.81	12.77	549.10	179.09
MO144-13	779.7	68.7	11.3	2839	0.0621	17.15	0.0090	4.22	0.25	20.03	16.62	57.87	2.45	61.14	10.75	191.29	193.27
MO144-14	620.3	39.2	15.8	3535	0.0887	11.71	0.0136	3.24	0.28	21.12	11.25	87.06	2.84	86.34	10.50	66.36	133.94
MO144-15	763.2	56.4	13.5	4337	0.0737	17.06	0.0089	3.61	0.21	16.69	16.67	57.24	2.08	72.18	12.68	600.16	180.48
MO144-16	1097.0	1116.9	1.0	1150	0.0924	20.14	0.0129	7.05	0.35	19.27	18.87	82.67	5.87	89.70	18.72	281.05	215.89
MO144-17	427.9	18.0	23.8	2317	0.0704	21.02	0.0088	3.10	0.15	17.31	20.79	56.69	1.76	69.06	14.91	521.60	228.06
MO144-18	273.8	30.8	8.9	1355	0.0659	16.98	0.0086	7.34	0.43	18.04	15.32	55.30	4.07	64.77	11.30	430.30	170.69
MO144-19	346.0	17.3	20.0	1462	0.0621	29.30	0.0091	3.57	0.12	20.09	29.08	58.10	2.08	61.21	18.32	184.48	338.60

Table 1 (Continued). LA-MC-ICPMS U-Pb zircon data of samples from the Atoyac and Zihuatanejo transects.

	Concentration				Isotopic Ratio							Apparent ages					
Sample	U (ppm)	Th (ppm)	U/Th	$U^{206}Pb_m$/$^{204}Pb_c$	^{207}Pb/^{235}U	±%	^{206}Pb/^{238}U	±%	Error corr	^{206}Pb/^{207}U	±%	^{206}Pb/^{238}U	±Ma	^{207}Pb/^{235}U	±Ma	^{207}Pb/^{206}Pb	±Ma
MO144-20	629.5	59.2	10.6	1077	0.0723	24.55	0.0088	5.18	0.21	16.83	24.00	56.62	2.95	70.86	17.86	582.75	260.58
MO145																	
MO145-1	93.6	68.5	1.4	224	0.1249	65.17	0.0101	11.84	0.18	11.16	64.08	64.80	7.71	119.47	79.43	1417.76	612.59
MO145-3	31.9	15.3	2.1	117	0.0331	63.68	0.0057	8.57	0.13	23.81	63.10	36.79	3.16	33.10	21.20	NA	NA
MO145-4	81.6	42.5	1.9	336	0.0283	109.6	0.0060	15.42	0.14	29.30	108.6	38.67	5.98	28.35	31.06	NA	NA
MO145-5	113.5	41.7	2.7	249	0.0994	23.39	0.0057	5.83	0.25	7.96	22.65	36.88	2.16	96.27	23.35	2038.74	200.26
MO145-6	88.2	62.6	1.4	286	0.1230	40.18	0.0060	16.22	0.40	6.75	36.76	38.71	6.30	117.78	48.98	2323.86	315.04
MO145-8	142.7	60.4	2.4	1491	0.1642	23.69	0.0206	5.64	0.24	17.28	23.01	131.37	7.48	154.41	38.76	524.49	252.29
MO145-9	145.2	43.4	3.3	840	0.1698	77.78	0.0100	15.47	0.20	8.16	76.23	64.43	10.01	159.20	125.93	1993.86	677.53
MO145-10	89.1	20.9	4.3	654	0.1260	57.64	0.0097	15.11	0.26	10.65	55.63	62.46	9.47	120.53	71.22	1506.00	525.47
MO145-11	213.2	53.4	4.0	1350	0.0809	79.57	0.0093	10.75	0.14	15.83	78.84	59.62	6.43	79.02	63.37	714.01	837.54
MO145-12	87.4	57.7	1.5	1023	0.1291	46.58	0.0067	5.86	0.13	7.15	46.21	43.02	2.53	123.29	59.30	2225.11	400.23
MO145-13	89.6	46.7	1.9	251	0.1180	46.19	0.0060	18.66	0.40	7.05	42.26	38.77	7.25	113.27	53.89	2250.51	364.95
MO145-14	133.2	44.5	3.0	8150	1.6379	5.26	0.1619	1.22	0.23	13.63	5.12	967.23	12.73	984.91	83.93	1024.52	51.77
MO145-15	55.5	25.5	2.2	254	0.1661	44.77	0.0060	10.25	0.23	4.95	43.58	38.33	3.94	155.99	72.82	2842.03	355.16
MO145-16	47.3	17.3	2.7	215	0.0465	45.12	0.0061	6.74	0.15	18.11	44.62	39.29	2.65	46.19	21.11	420.93	498.04
MO145-17	49.1	17.3	2.8	153	0.0194	118.2	0.0056	20.39	0.17	39.56	116.5	35.85	7.33	19.55	23.07	NA	NA
MO145-18	95.0	39.5	2.4	299	0.1501	49.70	0.0062	20.97	0.42	5.66	45.06	39.60	8.32	142.04	73.08	2622.43	374.74
MO145-20	161.6	61.0	2.6	356	0.1371	39.01	0.0161	8.28	0.21	16.24	38.12	103.26	8.61	130.48	52.91	659.95	408.56
MO145-23	124.6	48.5	2.6	345	0.0915	63.90	0.0090	5.34	0.08	13.62	63.67	58.04	3.11	88.92	57.71	1024.88	644.11
MO145-24	115.7	51.4	2.2	363	0.1222	22.42	0.0066	9.13	0.41	7.45	20.48	42.42	3.89	117.11	27.46	2154.75	178.71
MO145-25	124.4	34.5	3.6	440	0.2204	276.9	0.0090	5.05	0.02	5.63	276.3	57.74	2.93	202.24	483.69	2631.14	2300.25
MO145-26	90.5	102.8	0.9	162	0.1017	31.76	0.0064	6.47	0.20	8.73	31.09	41.40	2.68	98.37	32.28	1872.39	280.35
MO145-27	143.5	31.4	4.6	303	0.0868	56.56	0.0065	3.28	0.06	10.26	56.46	41.53	1.37	84.55	48.68	1575.87	528.46

Two tectonostratigraphic terrane configurations of south Mexico are widely used (Campa and Coney, 1983; Sedlock *et al*., 1993). Names are different and some of the limits are slightly different, but both are essentially similar. Nevertheless, in the case of the Campa and Coney (1983) configuration, the Xolapa terrane is juxtaposed against the Guerrero Terrane as well as the Mixteca and Oaxaca terranes. In contrast, the Sedlock *et al*. (1993) configuration shows the Xolapa Terrane juxtaposed only against the Mixteca and Oaxaca terranes. Location of the true limits of Xolapa is not only of geometric significance, but it has important implications for the origin and geologic evolution of Xolapa and southern Mexico. Our data indicate that along the Atoyac transect, granitic magmas had significant interactions with older continental rocks similar to those of the Xolapa or Acatlán complexes. This fact suggests that the Atoyac region most probably forms part of the Xolapa terrane and not of the Guerrero terrane as suggested by the configuration of Sedlock *et al*. (1993); this is supported by Nd model ages around 0.8 Ga (Schaaf *et al*., 1995). Based on our data, we believe that the boundary between the Guerrero and Xolapa terranes is located between these studied transects, which does not support a boundary between Chatino (Xolapa) and Nahuatl (Guerrero) terranes located closely west of Acapulco as proposed by Sedlock *et al*. (1993).

These new age data provide additional information regarding coastal arc magmatism along the Pacific margin of Mexico during the Cenozoic. The ages presented herein provide strong evidence for a protracted episode of Cordilleran style arc magmatism within the Xolapa complex for much of the Cenozoic, prior to the early Miocene.

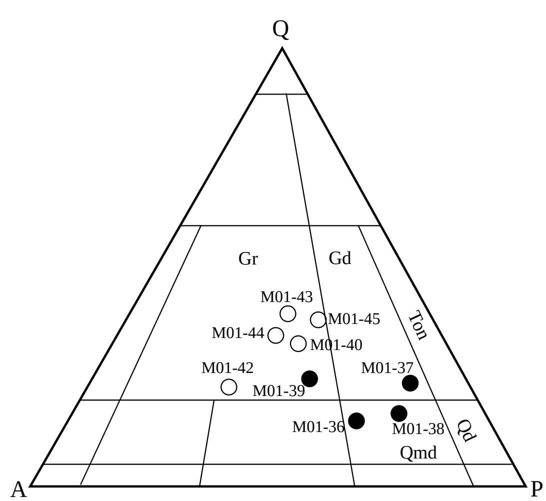

Figure 4. Streckeisen (1976) diagram showing modal proportion of studied samples. Atoyac samples plotted as empty circle. Zihuatanejo transect plotted as solid circles. Gr: granite, Gd: granodiorite, Ton: tonalite, Qmd: quartzmonzodiorite, and Qd: quartzdiorite.

Table 2. Sample location and summary of U-Pb ages.

Sample	Coordinates		Rock Type	Age * (Ma)	Other ages (fission track)
Zihuatanejo transect					
MO136	N 17º 51’ 08.6’’	W 101º 22’ 51.4’’	Bt-Hbl quartz-monzodiorite	41.8 ± 1.4 Ma	
MO137	N 17º 56’ 04.5’’	W 101º 17’ 04.8’’	Bt granodiote	43.4 ± 1.6 Ma	28.4 ± 4.4 Ma
MO138	N 17º 56’ 59.6’’	W 101º 16’ 29.4’’	Bt-Hbl quartz-monzodiorite	40.8 ± 1.4 Ma	
MO139	N 17º 36’ 28.8’’	W 101º 27’ 51.8’’	Bt granite	41.8 ± 4.6 Ma	
Atoyac de Álvarez transect					
MO140	N 17º 13’ 54.6’’	W 100º 24’ 47.7’’	Granite	53.5 ± 1.9 Ma	31.7 ± 5.3 Ma
MO141	N 17º 14’ 59.7’’	W 100º 21’ 59.3’’	Granite	52.7 ± 1.9 Ma *326 Ma*	
MO142	N 17º 19’ 19.4’’	W 100º 14’ 56.7’’	Bt granite	57.3 ± 1.9 Ma *72–74 (2), 90–92 (2), 385, 1085 Ma*	18.7 ± 2.0 Ma
MO143	N 17º 22’ 03.4’’	W 100º 12’ 09.6’’	Bt granite	54.4 ± 1.7 Ma *102–106 (3), 143–155 (3), 960, 1848 Ma*	
MO144	N 17º 24’ 48.4’’	W 100º 11’ 51.0’’	Bt granite	57.0 ± 2.1 Ma *83-87(4) Ma*	
MO145	N 17º 09’ 08.9’’	W 100º 24’ 27.7’’	Bt-granite (deformed)	40.2 ± 1.4 Ma *58-64 (6), 103,111, 1024 Ma*	22.5 ± 2.2 Ma

*Ages in italics are inherited ages.

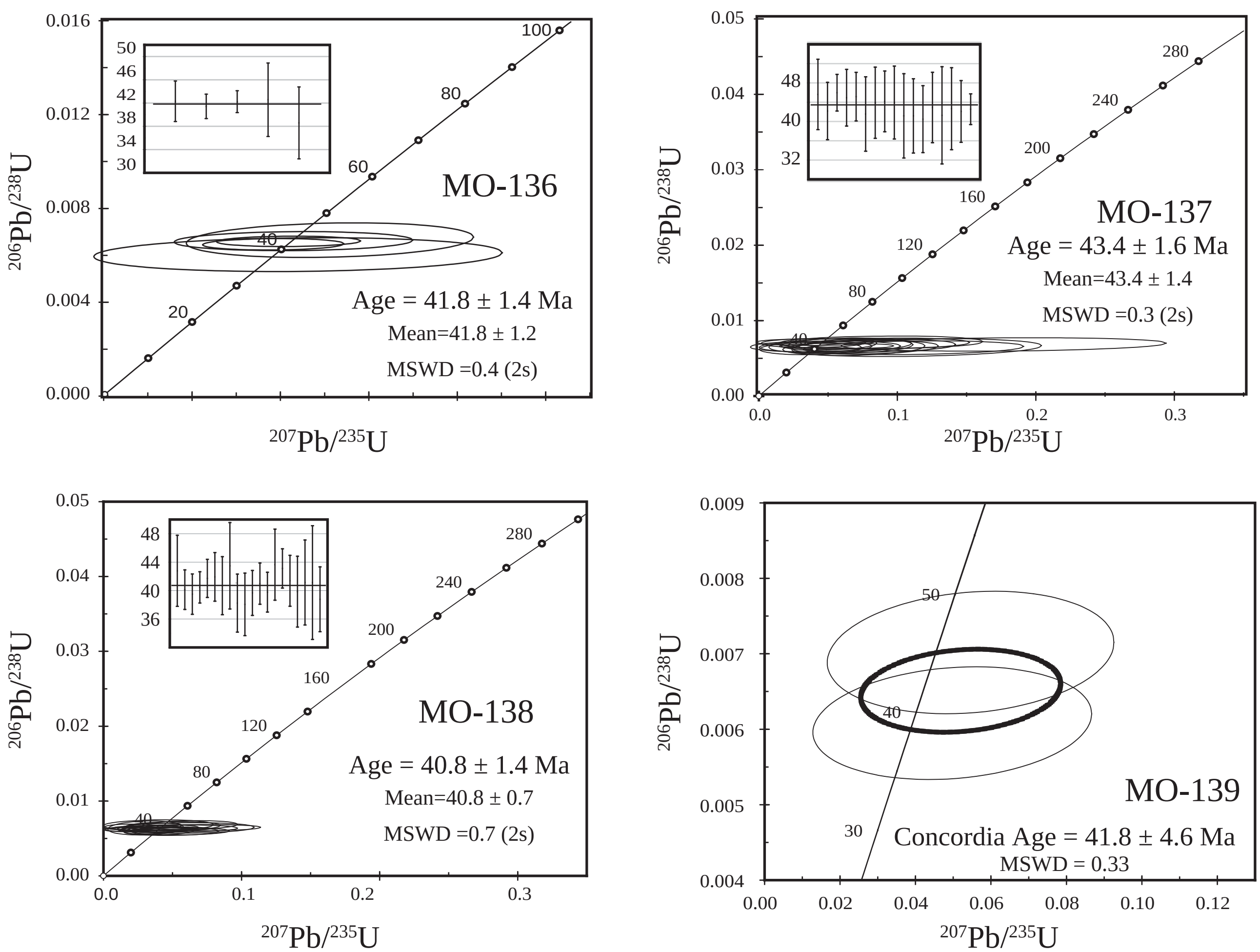

Figure 5. U-Pb ages for the Zihuatanejo transect.

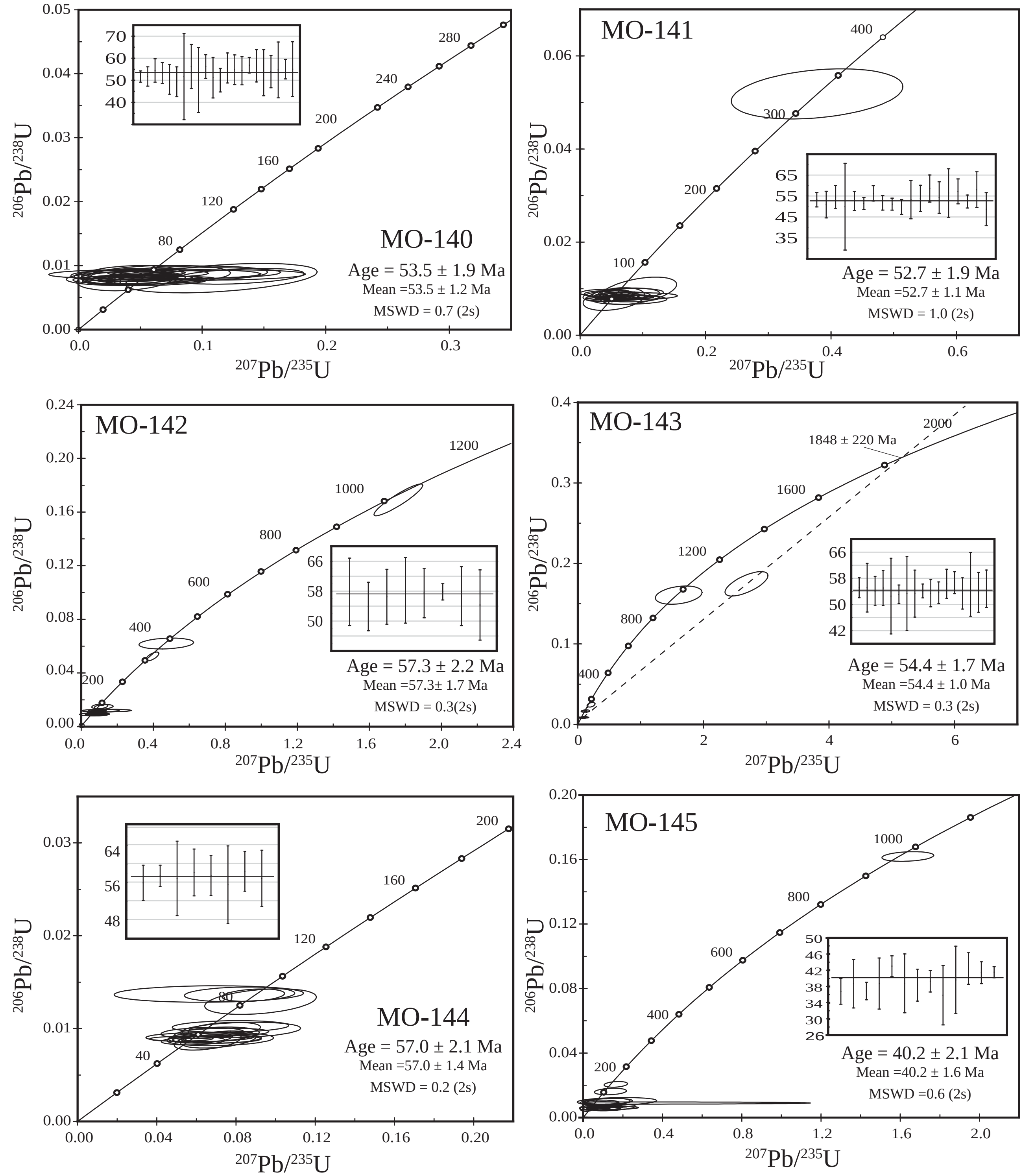

Figure 6. U-Pb ages for the Atoyac de Álvarez transect.

The Eocene-Oligocene post-kinematic (*i.e.*, largely undeformed) arc-related intrusives within the Sierra Madre del Sur formed during a ~20 Ma high flux magmatic event, that is typical for Cordilleran arcs (*e.g.*, Ducea and Barton, 2007). If about half of the width of the Xolapa Complex is occupied by these plutons, as indicated by available geologic mapping, apparent intrusive fluxes for this flare-up event are ~800–1000 km^2/m.y., comparable to the largest flare-up events in the Cordillera, such as the Late Cretaceous event that built much of the Sierra Nevada (Ducea, 2001), or the Eocene flare-up of the Coast Mountains batholith (Gehrels *et al.*, 2007).

ACKNOWLEDGEMENTS

Arizona LaserChron Center is partially supported by NSF Instrumentation and Facilities Program grant (NSF-EAR 0443387). We would like to thank Peter Schaaf, Fernando Barra, Luigi Solari and an anonymous reviewer for their constructive comments and suggestions on the manuscript.

REFERENCES

Campa, M.F., Coney, P.J., 1983, Tectono-stratigraphic terranes and mineral distributions in Mexico: Canadian Journal of Earth Sciences, 20, 1040-1051.

Centeno-García, E., Ruiz, J., Coney, P.J., Patchett, P.J., Ortega-Gutiérrez, F., 1993, Guerrero terrane of Mexico: its role in the Southern Cordillera from new geochemical data: Geology, 21, 419–422.

Coney, P.J., 1983, Un modelo tectónico de México y sus relaciones con América del Norte, América del Sur, y el Caribe: Revista del Instituto Mexicano del Petróleo, 15, 6-15.

Coney, P.J., Campa, M.F., 1987, Folio of the lithotectonic terrane maps of the North American Cordillera: United States Geological Survey, Miscellaneous Field Studies, Map MF 1874-D.

Corona-Chávez, P., Poli, S., Bigioggero, B., 2006, Syn-deformational migmatites and magmatic-arc metamorphism in the Xolapa Complex, southern Mexico: Journal of Metamorphic Geology, 24, 169-192.

De Cserna, Z., 1965, Reconocimiento geológico en la Sierra Madre del Sur de México, entre Chilpancingo y Acapulco: Universidad Nacional Autónoma de México, Instituto de Geología, Boletín, 62, 1–77.

Ducea, M.N., 2001, The California arc: Thick granitic batholiths, eclogitic residues, lithospheric-scale thrusting, and magmatic flare-ups: GSA Today, 11, 4-10.

Ducea, M.N., Barton, M.D., 2007, Temporal and spatial isotopic patterns in Cordilleran arcs and tectonic implications: Geology, 35, 1047-1050.

Ducea, M.N., Gehrels, G.E., Shoemaker, S., Ruiz, J. Valencia, V.A., 2004, Geological evolution of the Xolapa Complex, Southern Mexico. Evidence from U-Pb zircon geochronology: Geological Society of America Bulletin, 116, 1016-1025.

Gehrels, G.E., Valencia, V.A., Ruiz, J., 2008, Enhanced precision, accuracy, efficiency, and spatial resolution of U-Pb ages by laser ablation–multicollector–inductively coupled plasma–mass spectrometry: Geochemistry, Geophysics, Geosystems, 9, Q03017, doi:10.1029/2007GC001805.

Guerrero-García, J.C., 1975, Contributions to paleomagnetism and Rb-Sr geochronology: Dallas, University of Texas, Ph.D. thesis, 131p.

Herrmann, U.R., Nelson, B.K., Ratschbacher, L., 1994, The origin of a terrane: U /Pb zircon geochronology and tectonic evolution of the Xolapa complex (southern Mexico): Tectonics, 13, 455-474.

Keppie, J.D., Sandberg, C.A., Miller, B.V., Sánchez- Zavala, J.L., Nance, R.D., Poole, F.G., 2004, Implications of latest Pennsylvanian to middle Permian paleontological and U-Pb SHRIMP data from the Tecomate Formation to re-dating tectonothermal events in the Acatlán Complex, southern México: International Geology Review, 46, 745–753.

Meschede, M., Frisch, W., Herrmann, U. R., Ratschbacher, L., 1997, Stress transmission across an active plate boundary: an example from southern México: Tectonophysics, 266, 81-100.

Morán-Zenteno, D.J., 1992, Investigationes isotópicas de Rb-Sr y Sm-Nd en rocas cristalinas de la region de Tierra Colorada-Acapulco-Cruz Grande, Estado de Guerrero: Mexico D. F, Universidad Nacional Autonoma de México UACPyP, Ph.D. thesis, 187 p.

Morán-Zenteno, D., Corona-Chávez, P., Tolson, G., 1996, Uplift and subduction erosion in southwestern Mexico since the Oligocene: pluton geobarometry constraints: Earth and Planetary Science Letters, 141, 51-65.

Morán-Zenteno, D.J., Tolson, G., Martínez-Serrano, R.G., Martiny, B., Schaaf, P., Silva-Romo, G., Macías-Romo, C., Alba-Aldave, L., Hernández-Bernal, M.S., Solís-Pichardo, G.N., 1999, Tertiary arc-magmatism of the Sierra Madre del Sur, Mexico, and its transition to the volcanic activity of the Trans-Mexican Volcanic Belt: Journal of South American Earth Sciences, 12, 513-535.

Ortega-Gutiérrez, F., Elías-Herrera, M., Reyes-Salas, M.A., Macías-Romo, C, Lopez, R., 1999, Late Ordovician-early Silurian continental collisional orogeny in southern Mexico and its bearing on Gondwana-Laurentia connections: Geology, 27, 719-722.

Ratschbacher, L., Riller, U., Meschede, M., Herrmann, U., Frisch, W., 1991, Second look at suspect terranes in southern Mexico: Geology, 19, 1233-1236.

Riller, U., Ratschbacher, L., Frisch, W., 1992, Left-lateral transtension along the Tierra Colorada deformation zone, northern margin of the Xolapa magmatic arc of southern Mexico: Journal of South American Earth Sciences, 5, 237-249.

Robinson, K.L., Gastil, R.G., Campa, M.F., Ramirez-Espinosa, J., 1989, Geochronology of basement and metasedimentary rocks in southern Mexico and their relation to metasedimentary rocks in Peninsular California: Geological Society of America Abstracts with Programs, 21, 135 p.

Rubatto, D., 2002, Zircon trace element geochemistry: partitioning with garnet and the link between U–Pb ages and metamorphism: Chemical Geology, 184, 123–138.

Schaaf, P., Morán-Zenteno, D.J., Hernández-Bernal, M.S., Solís-Pichardo, G., Tolson, G., Köhler, H., 1995, Paleogene continental margin truncation in southwestern Mexico: Geochronological evidence: Tectonics, 14, 1339–1350, doi: 10.1029/95TC01928.

Sedlock, R.L., Ortega-Gutiérrez, F., Speed, R.C., 1993, Tectonostratigraphic terranes and tectonic evolution of Mexico:. Geological Society of America, Special Paper 278, 180 p.

Solari, L.A., Torres de León, R., Hernández Pineda, G., Solé, J., Hernández-Treviño, T., Solís-Pichardo, G., 2007, Tectonic significance of Cretaceous–Tertiary magmatic and structural evolution of the northern margin of the Xolapa Complex, Tierra Colorada area, southern Mexico: Geological Society of America, Bulletin 119, 1265.

Stacey, J.S., Kramers, J.D., 1975, Approximation of terrestrial lead isotope evolution by a two-stage model: Earth and Planetary Sciences Letters, 26, 207-221.

Stein, G., Lapierre, H., Vidal, R., Monod, O., Zimassique J.-L., 1994, Petrology and geochemistry of some Late Mesozoic and Tertiary plutons: Journal of South American Earth Sciences, 7, 1–7.

Streckeisen, A., 1976, To each plutonic rock its proper name: Earth Science Reviews, 12, 1–33.

Talavera-Mendoza, O., Ruiz, J., Gehrels, G.E., Meza-Figueroa, D.M., Vega-Granillo, R., Campa-Uranga, M.F., 2005, U-Pb geochronology of the Acatlán Complex and implications for the Paleozoic paleogeography and tectonic evolution of southern Mexico: Earth and Planetary Science Letters, 235, 682–699, doi: 10.1016/j.epsl.2005.04.013.

Talavera-Mendoza, O.,Ruiz, J.,Gehrels, G.E.,Valencia, V.A.,Centeno-García, E., 2007, Detrital zircon U/Pb geochronology of southern Guerrero and western Mixteca arc successions (southern Mexico): New insights for the tectonic evolution of southwestern North America during the late Mesozoic: Geological Society of America Bulletin, 119, 1052-1065.

Tolson, G., Solís-Pichardo, G., Morán-Zenteno, D.J., Victoria-Morales, A., Hernandez-Treviño, T., 1993, Naturaleza petrográfica y estructural de las rocas cristalinas en la zona de contacto entre los terrenos Xolapa y Oaxaca, región de Santa María Huatulco, Oaxaca, *in* Delgado-Argote, L., Martín-Barajas, A. (eds.), Contribuciones a la Tectónica del Occidente de México: México, Unión Geofísica Mexicana, Monografía 1, 327–349.

Manuscript received: December 12, 2007
Corrected manuscript received: August 28, 2008
Manuscript accepted: August 26, 2008